Growth and Morphology Control of Silver Halide Nanoparticles in Templated Ag(I)-Coordinated Langmuir−Schaefer Films

Haofei Gong and Minghua Liu*

Laboratory of Colloid and Interface Science, Center for Molecular Science, Institute of Chemistry, Chinese Academy of Sciences, Beijing 100080, People's Republic of China

Received March 18, 2002. Revised Manuscript Received August 5, 2002

Growth and morphology control of silver halide nanoparticles in templated organized molecular films have been investigated. Instead of using conventional Langmuir−Blodgett (LB) films, in this paper silver (I) coordinated Langmuir−Schaefer (LS) films of coumarin 7 (which have no long alkyl chains) were used. The nanoparticles and their aggregation patterns were obtained in the film upon gas exposure and immersion in aqueous solutions. Because of the lack of long alkyl chains, the halide anion can easily penetrate into the Ag(I)-coordinated LS films to form nanoparticles, and the formed silver halide nanoparticles can be directly aggregated into various morphologies in the LS films. Upon exposing the Ag(I)-containing coumarin 7 LS films to HCl or I_2 gases, globular, cubic, dendrite, and nanorod morphologies of the silver halide were observed. The formation and aggregation processes of the nanoparticles in the LS films were monitored at intervals. Different morphologies were observed when immersing the Ag(I)-coordinated LS films into the aqueous solutions containing potassium halide. In the case of immersion into a KI solution, a nanowire of AgI was obtained. We have found that globular nanoparticles were always formed in the initial aggregation stage. Different morphologies such as cubic, dendrite, nanorod, and nanowire were obtained in subsequent reactions depending on the conditions. Directional aggregation was suggested for the formation of these morphology patterns. The Ag(I)-coordinated LS film revealed itself to be a good template for the in situ generation of a nanosized silver (I) halide with different morphologies.

1. Introduction

Recently, the investigation and preparation of inorganic nanoparticles and nanocrystals have been drawing considerable attention because of their wide applications in optoelectrical, magnetic, and catalytic fields.[1,2] In preparation of the nanoparticles, template-directed growth was found to be a powerful method and has been widely studied.[3−15] Among those studies on the formation of template-directed nanoparticles, various templates, such as self-assembly monolayer,[5] micelles,[6−8] vesicles,[9,10] Langmuir monolayer,[11−13] and Langmuir−Blodgett films[14,15] have been extensively used. Monolayer and Langmuir−Blodgett techniques are among the most effective ways in controlling the molecular orientation and packing at a molecular level.[16] Because the packing and the thickness of the molecular films can be fabricated in a controlled manner, Langmuir and Langmuir−Blodgett films can provide possible templates to control the nucleation and growth of organized inorganic nanoparticles. Metal nanoparticles have been generated in the organized LB films through γ-ray or photo reduction.[17,18] It is also expected that nanoparticles of the metal salt could be formed through the chemical reactions of the metal ion-containing LB films with external compounds. Although the reaction between the LB films and gases could easily progress, the reaction in aqueous solutions appeared to be hindered

* To whom correspondence should be addressed. Fax: 86-10-6256-9564. E-mail: liumh@infoc3.icas.ac.cn.

(1) Henglein, A. *Top. Curr. Chem.* **1998**, *143*, 133.
(2) Anders, P. R.; Averback, R. S.; Brown, W. W. L.; Brus, L. E.; Goddard, W. A.; Kaldor, A.; Louie, S. G.; Moskovits, M.; Percy, P. S.; Riley, S. J.; Siegel, R. W.; Spaepen, F.; Wang, Y. *J. Mater. Res.* **1989**, *4*, 704.
(3) Liu, C.; Zou, B.; Rondinone, A. J.; Zhang, Z. J. *J. Am. Chem. Soc.* **2001**, *123*, 4344.
(4) Gröhn, F.; Kim, G.; Bauer, B. J.; Amis, E. J. *Macromolecules* **2001**, *34*, 2179.
(5) (a) Nabok, A. V.; Richardson, T. *Langmuir* **1997**, *13*, 3198. (b) Chen, C. C.; Lin, J. J. *Adv. Mater.* **2001**, *13*, 136.
(6) Zhao, H.; Douglas, E. P.; Harrison, B. S.; Schanze, K. S. *Langmuir* **2001**, *17*, 8428.
(7) Pletil, J.; Pospíil, H.; Kadlec, J. K. P.; Tuzar, Z.; Cubitt, R. *Langmuir* **2001**, *17*, 6699.
(8) Cason, J. P.; Miller, M. E.; Thompson, J. B.; Roberts, C. B. *J. Phys. Chem. B* **2001**, *105*, 2297.
(9) Jiang, X.; Xie, Y.; Lu, J.; Zhu, L.; He, W.; Qian, Y. *J. Mater. Chem.* **2001**, *11*, 1775.
(10) Korgel, B. A.; Monbouquette, H. G. *Langmuir* **2000**, *16*, 3588.
(11) Brown, J. J.; Porter, J. A.; Daghlian, C. P.; Gibson, U. J. *Langmuir* **2001**, *17*, 7966.
(12) Lu, L.; Cui, H.; Li, W.; Zhang, H.; Xi, S. *Chem. Mater.* **2001**, *13*, 325.
(13) Henrichs, S.; Collier, C. P.; Saykally, R. J.; Shen, Y. R.; Heath, J. R. *J. Am. Chem. Soc.* **2000**, *122*, 4077.
(14) Guo, S.; Konopny, L.; Popovitz-Biro, R.; Cohen, H.; Porteanu, H.; Lifshitz, E.; Lahav, M. *J. Am. Chem. Soc.* **1999**, *121*, 9589.
(15) Torimoto, T.; Tsumura, N.; Miyake, M.; Nishizawa, M.; Sakata, T.; Mori, H.; Yoneyama, H. *Langmuir* **1999**, *15*, 1853.
(16) Zasadzinski, J. A.; Viswanathan, R.; Madsen, L.; Garnaes, J.; Schwartz, D. K. *Science* **1994**, *263*, 1726.
(17) Huang, H. H.; Ni, X. P.; Loy, G. L.; Chem, C. H.; Tan, K. L.; Loh, F. C.; Deng, J. F.; Xu, G. Q. *Langmuir* **1996**, *12*, 909.
(18) Talham, D. R. *Langmuir* **1998**, *14*, 708.

10.1021/cm020232s CCC: $22.00 © 2002 American Chemical Society
Published on Web 10/15/2002

in many cases. This is because in order to fabricate the LB films amphiphiles with long alkyl chains are usually needed. However, because of a strong hydrophobic property of the alkyl chain, hydrated anions or cations can hardly penetrate into the LB films, which in turn hinder the growth of the nanoparticles using the ion-exchange method in solution. In addition, the substituted long alkyl chain in the nucleation center will possibly block the diffusion of the generated nanoparticles and make it impossible to form large aggregations of the nanostructured materials.[19,20] To avoid such disadvantages, LB films which contained no long alkyl chains were desired. Previously, we have reported that a series of benzimidazole derivatives, although having shorter or even no alkyl chains, could form stable monolayers on the aqueous subphase containing $AgNO_3$.[21−23] It has been confirmed that the monolayer formation was attributed to the in situ coordination between the benzimidazole and Ag(I), and the Ag(I)-coordinated complex monolayers can be transferred by the Langmuir−Schaefer method to form an ordered LS film. Because this LS film contains no long alkyl chains, it is possible to use the LS film to grow the nanoparticles of silver halide in a controlled manner either in gases or in aqueous solutions.

On the other hand, the shape or the morphology of nanoparticles together with their aggregations were as important as their size.[24−27]Although some examples of the shape or morphology control of the metal or inorganic nanoparticles in solutions were reported,[28−30] their control in ultrathin films has been less investigated. From the viewpoints of application, the in situ control of the shape and morphology of the inorganic nanoparticles or nanocrystals in ultrathin films was extremely important for adjusting the optical and catalytic properties of the materials. On the basis of these considerations, in this paper we have investigated the growth, aggregation, and morphological control of the nanoparticles in a templated ordered molecular film fabricated from 3-(2′-benzimidazolyl)-7-*N*,*N*-diethyl-aminocoumarin (CUM7). The choice of CUM7 is because it has no long alkyl chain and also can form an ordered Ag(I)-containing LS film on solid substrates.

2. Experimental Section

The compound used in the work was coumarin 7, 3-(2′-benzimidazolyl)-7-*N*,*N*-diethyl-aminocoumarin (abbreviated as CUM7). CUM7 was purchased from ACROS and was of laser grade (>99%). $AgNO_3$ used in the subphase was recrystallized from mixed ethanol/water solution. KCl, KBr, KI, hydrochloric acid, and I_2 were all commercially available analytical reagents and used as received. Milli-Q purified water (18 MΩ cm) was used in all the cases.

Film depositions were carried out on a KSV mini trough (Helsinki, Finland). A monolayer of CUM7 was formed by spreading its chloroform solution (10^{-3} mol L^{-1}) onto the aqueous subphases containing 0.01 M of $AgNO_3$. The film was deposited on the freshly washed silicon wafer as a Langmuir−Schaefer film by the horizontal lifting method.[21] The surface pressure was kept at 10 mN/m. AgCl nanostructures were formed by simply exposing the Ag(I)-containing ultrathin films to HCl gas or immersing them in the 0.01 M KCl solution for different times at room temperature (ca. 20 °C). For AgI, the films were exposed to I_2 gas or immersing them in the 0.01 M KI solution. I_2 gas was obtained by heating the solid I_2. AgBr nanoparticles were fabricated by the reaction of the LS film with the 0.01 M KBr solution.

The LS films of Ag(I)-coordinated CUM7 were deposited on the quartz, carbon-coated Cu grids, and silicon wafer for UV−Vis spectra, TEM, and FESEM observations, respectively. The films were washed with water before TEM observations in the gas exposure process. Transmission electron microscope (TEM) observations were carried out on a Tacnai 20 (fei & philips). Field emission scanning electron microscopy (FESEM) was performed on the JSM-6301F scanning microscope. UV−Vis spectra of the ultrathin films were measured with a JASCO UV-530 spectrophotometer. X-ray photoelectron spectra (XPS) were measured with a VG Scientific ESCALAB 220-IXL spectrometer using Al Kα as the excitation source (1486.6 eV).

3. Results and Discussion

3.1. Possibility of Generating the AgX Nanoparticles in the Langmuir-Schaefer Films through Chemical Reactions. Previously, we have found that CUM7, although having no long alkyl chains, can form stable monolayers at the air/water interface under the inducement of a Ag(I) ion in the subphase. It has been confirmed that the monolayer was formed through the in situ coordination between the benzimidazole and Ag(I) ion. Further, we have found that the monolayer formed at the air/water interface can be transferred onto a solid substrate to form an ordered LS film.[21] Upon using this film as a template, nanoparticles of AgCl and AgI can be generated through the reaction of the film with HCl or I_2 gas, or immersing the film in aqueous KCl and KI solutions.

Figure 1a shows the UV−Vis spectral changes of the transferred ultrathin film on quartz plates upon exposure to HCl. The CUM7−Ag(I) complex LS film showed its absorption band at 440 nm. Upon exposure to HCl gas for 1 min, an obvious spectral change was observed, indicating that the coordination between CUM7 and Ag(I) might be cleaved due to the production of AgCl in the film. When the LS film was exposed to I_2 gas, a similar spectral change was observed as shown in Figure 1b.

Figure 1c shows the spectral changes of the LS films upon their immersion in the concentrated KCl solution. The intensity of the whole spectra increased successively within the 52 min of immersion in the KCl solution. The shoulder band at 384 nm disappeared, while the band at 461 nm appeared gradually, indicating the formation of AgCl in the film. The similar spectral changes were observed in the KI solution, as shown in Figure 1d. The intensity of the absorption band at 433 nm was increased and its position blue-shifted successively with the increase of immersion time, suggesting the

(19) Tang, R.; Tai, Z. *Langmuir* **1997**, *13*, 5204.
(20) Heywood, B. R.; Mann, S. *Langmuir* **1992**, *8*, 1492.
(21) Gong, H.; Liu, M. *Langmuir* **2001**, *17*, 6228.
(22) Liu, M.; Kira, A.; Nakahara, H. *Langmuir* **1997**, *13*, 4807.
(23) Cai, J.; Liu, M.; Dong, C.; Li, J.; Tang, J.; Jiang, L. *Colloids and Surf., A* **2000**, *175*, 165.
(24) Zhu, J.; Liu, S.; Palchik, O.; Koltypin, Y.; Gedanken, A. *Langmuir* **2000**, *16*, 6396.
(25) Zhou, Y.; Yu, S. H.; Wang, C. Y.; Li, X. G.; Zhu, Y. R.; Chen, Z. Y. *Adv. Mater.* **1999**, *11*, 850.
(26) Zhan, J. H.; Yang, X. G.; Wang, D. W.; Li, S. D.; Xie, Y.; Xia, Y.; Qian, Y. *Adv. Mater.* **2000**, *12*, 1348.
(27) Xie, Y.; Huang, J.; Li, B.; Liu, Y.; Qian, Y. *Adv. Mater.* **2000**, *12*, 1523.
(28) Qi, L.; Cölfen, H.; Antonietti, M. *Angew. Chem., Int. Ed.* **2000**, *39*, 604.
(29) Qi, L.; Cölfen, H.; Antonietti, M. *Chem. Mater.* **2000**, *12*, 2392.
(30) Heywood, B. R.; Mann, S. *J. Am. Chem. Soc.* **1992**, *114*, 4681.

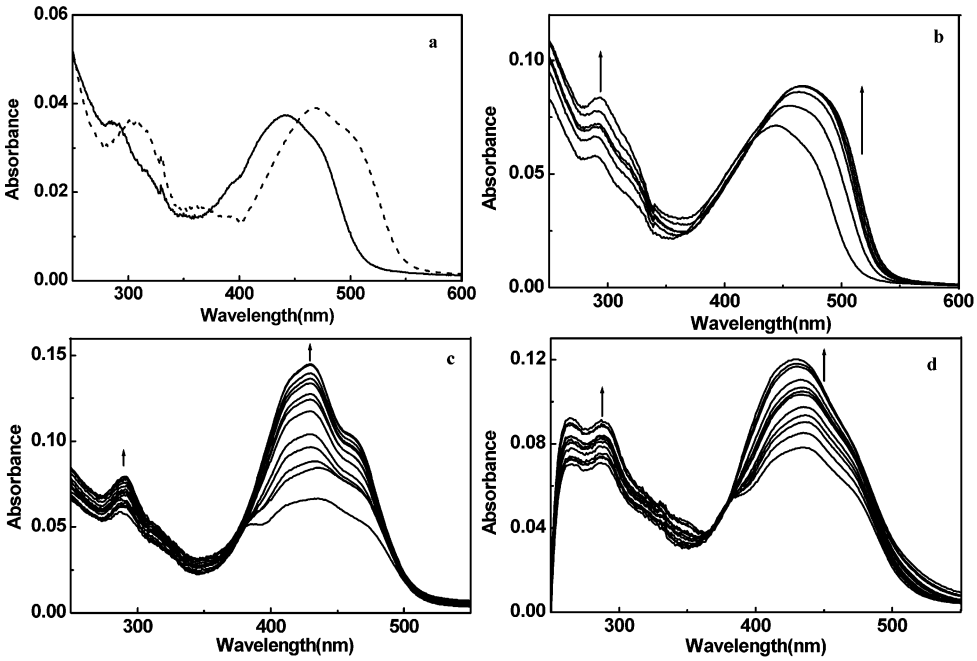

Figure 1. Absorption spectra of the LS film of coumarin 7 transferred on the subphase of 0.01 M of $AgNO_3$: (a) before (solid line) and after (dashed line) its exposure to HCl gas for 1 min; (b) before and after exposing it to hot I_2 gas for 0.5, 1, 1.5, 2, and 2.5 min; (c) after immersing it in the 0.01 M KCl solution for 0, 4, 8, ..., and 52 min; and (d) after immersing it in the 0.01 M KI solution for 0, 4, 8, ..., and 44 min.

unbinding of the CUM 7 to Ag(I), or the formation of AgI: $Ag(I) + I^- \rightarrow AgI$.

It can be clearly seen that when LS films were exposed to HCl or I_2 gas, or immersed into KCl or KI solutions, obvious spectral changes could be observed. However, the details of the spectral changes were different: in the case of gas exposure, a large red shift of the absorption was observed. This was due to the reaction of CUM 7 with the gases and the formation of AgX nanoparticles.[31] While in solution, the spectral changes reflected only the production of AgCl or AgI nanoparticles.

To confirm the formation of AgCl and AgI in the LS films, X-ray photoelectron spectrometry (XPS) was performed on the Ag(I)−CUM7 LS films after exposing the film to gases or immersing it in a solution. After exposing the film to HCl gas for 3 min, binding energies of Cl 2p were observed at 197.6 eV,[32] which is very close to the reported value for Cl 2p in AgCl, 197.5 eV,[33] confirming the formation of AgCl in the film. The binding energies of Ag3d5/2 and Ag3d3/2 were found at 367.4 and 373.3 eV, which is a low energy shift compared with the film before gas exposure.[21] This indicated the cleavage of a Ag(I)−imidazole coordination bond and the simultaneous formation of AgCl. Similar results were obtained in the formation of AgI in the LS film after immersion in the 0.01 M KI solution for 42 h. The binding energies of Ag3d5/2 and I3d5/2 were found at 368.1 and 619.5 eV, respectively, which were very close to the reported binding energies of AgI.[34]

3.2. Generation of AgCl Nanoparticles and Control of the Morphology. As discussed above, by exposing the LS film of CUM7−Ag(I) to HCl or dipping it into KCl, AgCl was formed on the film. To detect the formation of AgCl nanoparticles generated in the film, TEM or SEM observations were performed after exposing the film to HCl gas or immersing it in a KCl solution at intervals.

Figure 2 shows the TEM images of AgCl nanoparticles at consecutive exposure times. Upon exposure of the LS film to HCl gas for 10 s, globular AgCl nanoparticles with a diameter of 5−10 nm were observed. The morphology and the size of the particles changed with the exposure time. Upon exposure to HCl for 30 s, cubic particles of AgCl appeared in the film. These cubic particles grew larger with increased exposure time. They grew from 100 nm with 30 s of exposure to 150 nm in 1 min of exposure. Careful observation of the cubic AgCl nanoparticles revealed that these cubic particles were formed by directional aggregation of many smaller globular nanoparticles (Figure 2c).[29,35−37] An interesting discovery was observed when the film was exposed to HCl gas for 3 min, where the transmission electron micrograph showed a dendrite morphology. The dendrites were formed by the aggregation of numerous globular AgCl nanoparticles, because some obvious AgCl nanoparticles were clearly seen near the branches of the dendrites. This large and random supramolecular structure of AgCl nanoparticles was a universal morphology observed under the rapid growth model,[38−40] in which the nucleation of the nanoparticle was very much quicker than the diffusion of the particle

(31) It has been found that pure CUM7 film showed a large red shift upon exposure to HCl gas accompanying an obvious color change. When the film was further exposed to NH_3 gas, the color could be returned.

(32) All these values were calculated using C1s = 284.6 eV as a standard.

(33) Kishi, K.; Ikeda, S. *Bull. Chem. Soc. Jpn.* **1973**, *46*, 341.

(34) Gaarenstroom, S. W.; Winograd, N. *J. Chem. Phys.* **1977**, *67*, 3500.

(35) Zhang, D.; Qi, L.; Ma, J.; Cheng, H. *Chem. Mater.* **2001**, *13*, 2753.

(36) Qi, L.; Ma, J.; Cheng, H.; Zhao, Z. *J. Phys. Chem. B* **1997**, *101*, 3460.

(37) Cölfen, H.; Antonietti, M. *Langmuir* **1998**, *14*, 582.

(38) Selvan, S. T. *Chem. Commun.* **1998**, 351.

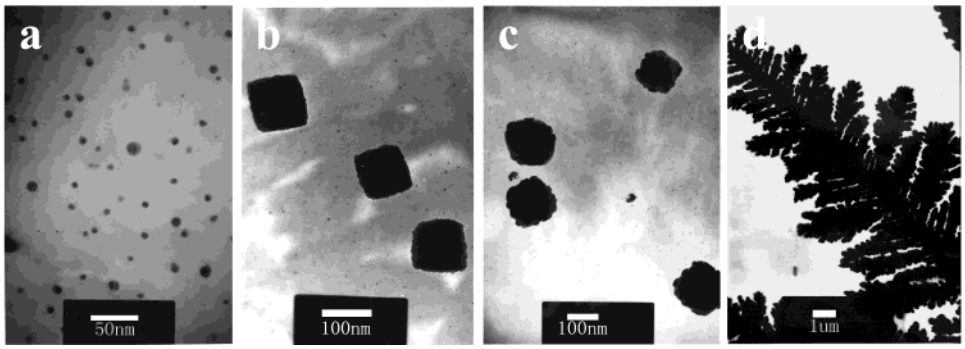

Figure 2. Transmission electron micrographs of the CUM7−Ag(I) complexed film under HCl gas exposure for (a) 10 s; (b) 30 s; (c) 1 min; and (d) 3 min. The films were washed with water before TEM observations.

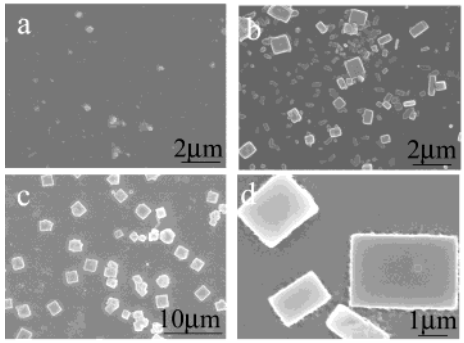

Figure 3. Scanning electron micrographs of the CUM7−Ag(I) complex film upon immersion in the KCl solution (0.01 M) for (a) 10 min; (b) 1 h; (c) 18 h; and (d) 42 h.

and then these generated particles stuck to each other to form the elegant tree.

When the film was dipped into the aqueous KCl solution different morphologies were observed. In our experiments, two layers of thin CUM7−Ag(I) film were transferred onto the silicon wafer and immersed in the 0.01 M KCl solution for different times. Figure 3 shows the SEM images of the AgCl nanoparticles. The first 10 min of immersion generated globular nanoparticles with a diameter of about 300 nm. The morphology and dimension of the particles changed with the increasing of immersion time. Figure 3b to 3d shows the images of nanoparticles with immersion times of 1 h, 18 h, and 42 h. We can find from these images that the morphology of the AgCl particles changed from globular to cubic, and the size of the particle increased. No significant morphological changes were observed when the immersion time exceeded 42 h except for a slight change in size.

From the above results, it is clear that both the gas penetration and ion exchange methods were efficient ways of forming inorganic nanoparticles and their aggregations. At the initial stages of the nanoparticle generation, globular morphology was always observed. Cubic AgCl aggregates could be observed both in gases and in solutions. Both of the cubic AgCl particles were found to be polycrystal (revealed to be so by electron diffraction), which further verified that the large AgCl particles were composed of directed aggregates of small crystalline nanoparticles. However, the dendrite morphology was not observed in the solution reaction process, indicating the nucleation and diffusion of the AgCl nanoparticles achieving equilibrium in solution was easier than in the gas-phase process.

It was noted that although cubic AgCl aggregates were formed in both processes, the cubic AgCl aggregates formed in the KCl solution have a more regular edge than those in the gas penetration process. This could be explained by the different nucleation and growth speeds of the two processes. Obviously, the AgCl generation speed in the gas penetration process was much faster than that in the ion penetration process. Several tens of seconds of HCl exposure generated the AgCl nanoparticles, and we could find a more dense distribution of the particles compared to those generated in the KCl solution. The newly generated nanoparticles tend to aggregate rapidly. We could see clearly in Figure 2c that the cubic particles were formed upon aggregation of the globular AgCl nanoparticles. However, in the case of immersion in the KCl solution, the reaction speed was dependent on the ion penetration speed, causing the edge of the cubelike aggregates to grow smoothly and the dimension of the cube to grow larger than it did in the gas penetration process. In the dilute aqueous KCl solution (e.g., 1 mM), no regular cubic particles of AgCl were observed. The SEM image showed only globular particles in the films either in the initial stage or after a very long time of immersion. The lack of sufficient counterions in the film prohibited the formation of cubic aggregates. This indicates that the concentration of counterions also plays an important role in the formation of AgCl nanoparticles. Therefore, by changing the concentration and immersion time, the morphologies of the AgCl nanoparticles can be controlled.

3.3. AgI Nanorods and Nanowires Formed in the Ultrathin Film. Figure 4 shows the TEM images of AgI nanoparticles and their aggregates grown in I_2 gas. Similar to the case of AgCl, separated nanoparticles with an average diameter of about 60 nm were observed in the initial 30 s of exposure. These nanoparticles were aggregated and the densities of the nanoparticles increased after exposure to I_2 for 3 min. Finally, the AgI nanoparticles aggregated directly to form nanorods when the film was exposed in I_2 gas for 5 min.

Upon immersion in the concentrated KI solution however, nanowires of AgI were observed after an extended immersion. Figure 5 shows the SEM images of the AgI formed in the 0.01 M KI solutions. Globular AgI nanoparticles were observed after the first 10 min of immersion as shown in Figure 5a. The globular AgI nanoparticles gradually aggregated into a wire-shaped

(39) Katzenelson, O.; Or, H. Z. H.; Avnir, D. *Chem. Eur. J.* **1996**, *2*, 174.
(40) Jacob, B.; Garik, P. *Nature* **1990**, *343*, 523.

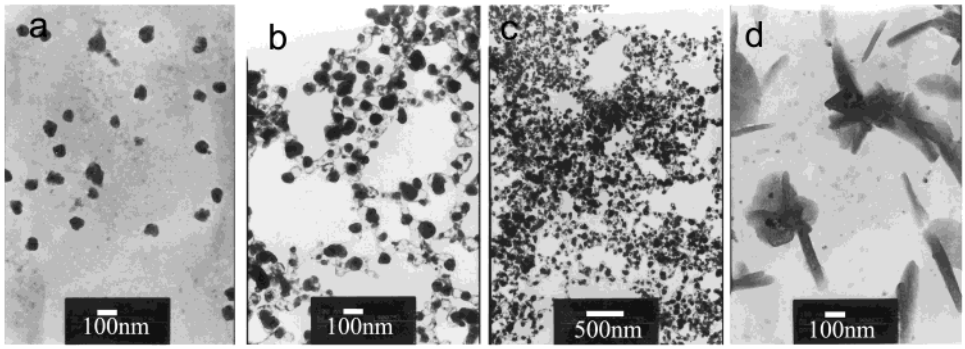

Figure 4. Transmission electron micrographs of the CUM7−Ag(I) complex film under hot I_2 gas exposure for (a) 30 s; (b) and (c) 3 min; and (d) 5 min. The films were washed with water before TEM observations.

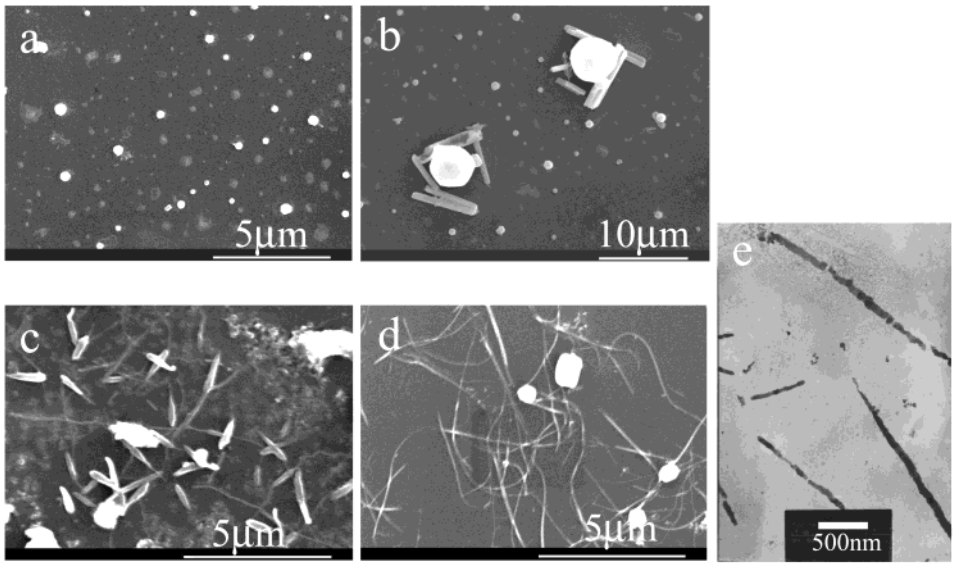

Figure 5. Scanning electron micrographs and transmission electron micrographs of the CUM7−Ag(I) complex film upon immersion in the KI solution (0.01 M) for (a) 10 min; (b) 1 h; (c) 18 h; (d) and (e) 42 h.

rod with the increasing immersion time in the KI solution, as can be clearly seen in Figure 5b and 5c. Finally, when the immersion time exceeded 40 h, these short nanorods formed elegant long nanowires as shown in Figure 5d. These nanowires have the diameter of about 70−200 nm and are several μm long. Further observations of TEM in Figure 5e showed that the nanowires were formed by aggregation of several sections of the short nanorods, which aggregated in a certain direction. Electron diffraction patterns showed that these nanowires were composed of polycrystal AgI.

The SEM and TEM observations clearly indicated that the nanorod and the nanowires are formed through a directional aggregation of nanoparticles.[35−37] In the initial stage, nanoparticles are always formed. These nanoparticles can further aggregate in a certain direction to form nanorods. In the case of gas exposure, the nanoparticles are formed rapidly and the subsequent directional aggregation is also quick. Owing to these, the growth of nanoparticles is stopped at the nanorod. In the solution process, due to the relative lower speed of the formation and aggregation of nanoparticles, the nanoparticles have enough time to grow in one direction to form a longer nanowire. In addition, in the solution reaction the surrounded water may help the aggregation of the AgI nanoparticles to form these nanowires.

3.4. Comparison of the AgX Formation in the Film. From the above results, it is clear that the morphologies of the AgX formed in the ultrathin film differ greatly depending on the forming process and the counteranion. In our cases, globular nanoparticles were always observed at the initial reaction stage, but the subsequent aggregation patterns were different. These different morphologies can be regarded as formed through directional aggregation. In the case of AgCl, cubic morphology was always observed either in the gas phase or in the solution reaction. But in the case of AgI, short nanorods or long nanowires were formed in the gas or solution reaction. These results further indicate that the aggregation habit also plays an important role in determining the final morphology.[36] We have also studied the formation of silver bromide nanoparticles in the same way in solution and only globular nanoparticles were observed.

The morphology of each silver halide generated in the two processes results in the conclusion that the aggregates in the ion penetration process were much larger and have a more clear edge than those in the gas penetration process. We attributed this to the different nucleation and aggregation speed between the two processes. In the ion penetration process, the nucleation and aggregation are slower than in the case of the gas process, which leads to a larger and clearer edge of the aggregates.

The template we used was a highly organized two-dimensional ultrathin film, which has a different ag-

gregation environment from that in solutions or other media. The ultrathin film we used was different from conventional LB films in that no long alkyl chain was contained in the film, making the further aggregation of inorganic nanoparticles easier, in addition to creating various morphologies. Although silver (I) coordinated CUM7 can also be obtained by coordination of CUM7 with $AgNO_3$ in methanol solutions, the formed coordination compound cannot dissolve in any organic solvents due to its polymeric nature. It therefore cannot be used to form a templated LS film. However, upon using the interfacial coordination method, an ordered templated LS film can be obtained. This method extended the monolayer forming materials to those molecules without long alkyl chains and facilitated the effective formation of inorganic nanoparticles and their organized aggregations in the ultrathin organic films.

4. Conclusions

Using an Ag(I)-coordinated Langmuir−Schaefer film, where the starting organic compounds have no long alkyl chains, silver halide nanoparticles have been grown in the ultrathin film either by exposure to gas or immersion into an aqueous KX solution. Globular nanoparticles were always formed in the initial stage using both methods. Dendrite morphology of AgCl nanoparticles could be obtained in the final stages of the HCl gas exposure. Although nanorods of AgI were formed in the gas-exposing method, AgI nanowires up to several micrometers long were obtained upon immersion into an aqueous KI solution. Only globular AgBr particles were formed in the film. The ion penetration process caused a larger and clearer edge of the aggregates. Directional aggregation processes and the aggregation habit of the AgX with different anions are found to play important roles in the formation of these morphologies. Our two-dimensional Ag(I)-coordinated LS film could serve as a good template for the in situ generation of nanosized inorganic materials with different morphologies.

Acknowledgment. This work was supported by the Major State Basic Research Development Program 973 (Grant G2000078103), Outstanding Youth Fund, National Natural Science Foundation, and the Fund of the Chinese Academy of Sciences.

CM020232S